HHS Public Access

Author manuscript

Biochem J. Author manuscript; available in PMC 2015 March 09.

Published in final edited form as:

Biochem J. 2008 October 15; 415(2): 225–232. doi:10.1042/BJ20080411.

Dipeptidyl-peptidase I does not functionally compensate for the loss of tripeptidyl-peptidase I in the neurodegenerative disease late-infantile neuronal ceroid lipofuscinosis

Kwi-Hye Kim[*,†], **Christine T. Pham**[‡], **David E. Sleat**[*,§], and **Peter Lobel**[*,§,1]

[*]Center for Advanced Biotechnology and Medicine, University of Medicine and Dentistry of New Jersey-Robert Wood Johnson Medical School, Piscataway, NJ 08854, U.S.A.

[†]Graduate Program in Molecular Biosciences, University of Medicine and Dentistry of New Jersey-Robert Wood Johnson Medical School, Piscataway, NJ 08854, U.S.A.

[‡]Division of Rheumatology, Department of Internal Medicine, Washington University, Saint Louis, MO 63110, U.S.A.

[§]Department of Pharmacology, University of Medicine and Dentistry of New Jersey-Robert Wood Johnson Medical School, Piscataway, NJ 08854, U.S.A.

Abstract

LINCL (late-infantile neuronal ceroid lipofuscinosis) is a fatal neurodegenerative disease resulting from mutations in the gene encoding the lysosomal protease TPPI (tripeptidyl-peptidase I). TPPI is expressed ubiquitously throughout the body but disease appears restricted to the brain. One explanation for the absence of peripheral pathology is that in tissues other than brain, other proteases may compensate for the loss of TPPI. One such candidate is another lysosomal aminopeptidase, DPPI (dipeptidyl-peptidase I), which appears to have overlapping substrate specificity with TPPI and is expressed at relatively low levels in brain. Compensation for the loss of TPPI by DPPI may have therapeutic implications for LINCL and, in the present study, we have investigated this possibility using mouse genetic models. Our rationale was that if DPPI could compensate for the loss of TPPI in peripheral tissues, then its absence should exacerbate disease in an LINCL mouse model but, conversely, increased CNS (central nervous system) expression of DPPI should ameliorate disease. By comparing TPPI and DPPI single mutants with a double mutant lacking both proteases, we found that the loss of DPPI had no effect on accumulation of storage material, disease severity or lifespan of the LINCL mouse. Transgenic expression of DPPI resulted in a ~2-fold increase in DPPI activity in the brain, but this had no significant effect on survival of the LINCL mouse. These results together indicate that DPPI cannot functionally compensate for the loss of TPPI. Therapeutic approaches to increase neuronal expression of DPPI are therefore unlikely to be effective for treatment of LINCL.

[1]To whom correspondence should be addressed (lobel@cabm.rutgers.edu).

Keywords

dipeptidyl-peptidase I (DPPI); lysosomal storage disorder; mouse model; protease; transgene; tripeptidyl-peptidase I (TPPI)

INTRODUCTION

The NCLs (neuronal ceroid lipofuscinoses) are a group of related, but genetically distinct, lysosomal storage disorders whose hallmarks include autofluorescent storage material within the cells of affected individuals and progressive death of neurons [1]. NCLs are inherited neurodegenerative diseases that primarily affect children and adolescents and they result in a range of clinical symptoms including seizures, blindness, mental regression, ataxia and premature death. Mutations in the *TPP1* gene [also called *CLN2* (ceroid lipofuscinosis neuronal 2)] are responsible for classical LINCL (late infantile neuronal ceroid lipofuscinosis) [2], one of the most common forms of NCL. LINCL typically presents at 2–4 years of age with seizures and the median life expectancy is ~12 years of age. LINCL is inevitably fatal and there is currently no treatment of demonstrated efficacy for affected individuals.

TPP1 encodes TPPI (tripeptidyl-peptidase I), a lysosomal enzyme that cleaves protein and peptide substrates at the third peptide bond downstream of an unsubstituted N-terminus [3]. A *Tpp1*-targeted mouse exhibits a severe neurodegenerative phenotype with no apparent visceral symptoms [4]. One intriguing characteristic of LINCL and the corresponding mouse model is that, despite the fact that TPPI is a widely distributed protease [2,5], the brain appears to be the only organ that is significantly affected by its deficiency. Bernardini and Warburton [6] have provided evidence that TPPI and the lysosomal enzyme DPPI (dipeptidyl-peptidase I; also called cathepsin C) have overlapping substrate specificity towards a model peptide and have proposed that DPPI can compensate for loss of TPPI in extraneuronal tissues. DPPI cleaves protein and peptide substrates at the second peptide bond downstream of an unsubstituted N-terminus and plays a role in cellular immunity by activating other proteases in the granules of immune cells [7–10]. Loss of DPPI activity arising from mutations in the *CTSC* gene (encoding DPPI) causes the human disease Papillon–Lefevre syndrome [11] and there is a $Ctsc^{-/-}$ mouse model [8]. DPPI is present in many cell types but is relatively low in brain.

If DPPI is capable of functionally substituting for TPPI, then therapies aimed towards increasing the expression of DPPI in brain could have significant potential for LINCL. In the present study, we have employed genetic approaches using gene targeted and transgenic mice to investigate the potential interplay between DPPI and TPPI in the development of neurological disease under physiological conditions.

EXPERIMENTAL

Animals

Mice were cared for in accordance with the guidelines of the NIH (National Institutes of Health) *Guide for the Care and Use of Laboratory Animals*. Animal protocols were

approved by the Institutional Animal Care and Use Committee of Robert Wood Johnson Medical School. Mice deficient in DPPI and TPPI, designated *Ctsc*$^{-/-}$ and *Tpp1*$^{-/-}$ respectively, have been described previously [4,8]. Genotyping of *Ctsc* was conducted by PCR analysis of tail DNA extracts using mouse *Ctsc* forward (5′-CCATCGAGTGGTGTTCCAGTTG-3′), mouse *Ctsc* reverse (5′-TCACCGAGCAGTTAATGTCGC-3′), LacZ forward (5′-GTGCCAGCGAATACCTGTTCC-3′) and LacZ reverse (5′-ACCCAGCTCGATGCAAAAATC-3′) primers that generate a 225 nt product from the wild-type allele (*Ctsc* primers) and a 400 nt product from the targeted allele (LacZ primers). Genotyping of TPPI-deficient mice was performed as described previously [4].

Generation of transgenic mice

A transgene for the overproduction of DPPI in the CNS (central nervous system) was constructed using the rat NSE (neuron-specific enolase) promoter (provided by Dr J. Gregor Sutcliffe, Department of Molecular Biology, Scripps Research Institute, La Jolla, CA, U.S.A.) and human CTSC cDNA sequences. The CTSC open reading frame was amplified by PCR reaction from an EST (expressed sequence tag) clone (IMAGE:5762611; Invitrogen) using primers CTSC-TgF (5′-CCGGTCTAGAATGGGTGCTGGGCCCTCCTT-3′) and CTSC-TgR (5′-AACCGCGGCCGCCTACAATTTAGGAATTGGTG-3′) that added XbaI and NotI sequences to the 5′ and 3′ ends respectively, which allowed subcloning to the equivalent sites in the plasmid vector pSTEC-1 [12] (provided by Dr Curt Sigmund, Center for Gene Therapy, University of Iowa, Iowa City, IA, U.S.A.). The NSE promoter sequence was amplified with SphI sites added to both 5′ and 3′ ends using primers NSE-F (5′-AATTGCATGCGAGCTCCTCCTCTGCTCGCCC-3′) and NSE-R (5′-CCGGGCATGCCTCGAGGACTGCAGACTCAGC-3′) and were inserted into the vector containing the CTSC coding sequence to create the transgene plasmid pNSE-CTSC. The SacI fragment of pNSE-CTSC containing the NSE promoter followed by a synthetic intron, the CTSC coding sequence, and an SV40 (simian virus 40) polyadenylation signal was gel-purified using GeneClean Turbo (Q-Biogene) and was used to create transgenic founders by Princeton University Animal Core Facilities in a B6SJL F1 background. Founders were crossed against *Tpp1*$^{-/-}$ animals in an isogenic C57BL/6 strain background and progeny containing the transgene were identified by Southern blotting analysis (see Figure 6B) where genomic DNA was digested with DraI and a 3.5 kb fragment was detected using a gel-purified 1.4 kb probe generated by digestion of the human CTSC cDNA sequence with NotI and XhoI. Transgene-positive mice were routinely genotyped by generation of a 540 nt fragment following PCR amplification of genomic DNA using primers Tg-F (5′-CCACTCCCAGTTCAATTACA-3′) and Tg-R (5′-CACATTCTCAGAGGCAGTTC-3′).

DPPI and TPPI enzyme assays

Mice were killed, perfused with ice-cold 1 × PBS and organs were collected and snap-frozen in liquid nitrogen and stored at −80°C until use. Tissue powders were prepared on dry ice using a Bessman tissue pulverizer. A portion of the tissue powders were suspended in 150 mM NaCl and 0.1% Triton X-100 (homogenization solution) at a ratio of 10 ml of solution per g of tissue and homogenized using a Polytron (Brinkmann Instruments). Duplicate

samples of the original homogenate as well as four additional 2-fold serial dilutions in homogenization solution were used for enzyme and protein assays. For DPPI enzyme activity assays, 10 μl of sample was added to 40 μl of 0.5 mM Gly-Arg-AMC (where AMC is 7-amino-4-methylcoumarin), 50 mM sodium acetate (pH 5.5), 150 mM NaCl, 0.1% Triton X-100, 2.5 mM EDTA and 5 mM dithiothreitol and incubated in the dark at 37 °C for 30 min with continuous shaking. For TPPI enzyme activity assays, 10 μl of sample was added to 40 μl of 0.25 mM Ala-Ala-Phe-AMC, 100 mM sodium acetate (pH 4.5), 150 mM NaCl and 0.1% Triton X-100 and incubated at 37°C in the dark for 1 h with continuous shaking. Enzymatic reactions were terminated by adding 100 μl of 0.1 M monochloroacetic acid, 0.13 M NaOH and 0.1 M acetic acid. The protein concentration was determined using the Advanced Protein Assay (Cytoskeleton). Enzyme activities and protein concentrations were calculated using replicate determinations from two to three dilutions in the linear range and enzyme activity was normalized to time and protein concentration.

Imaging of autofluorescent storage material

For imaging, 16–17-week-old mice were killed and transcardially perfused with ice-cold PBS followed by 4% (w/v) paraformaldehyde prepared in PBS. Brains and kidneys were removed and post-fixed in 4%(w/v) paraformaldehyde in PBS for 24 h at 4°C. Tissues were embedded in paraffin and 7 μm sagittal sections were collected. Deparaffinized sections were mounted on cover-slips with Vectashield mounting medium (Vector Laboratoriess) and viewed under a Olympus IX70 inverted microscope. Digital images were captured using IPLab software (BD Biosciences).

Immunodetection of SCMAS (subunit c of mitochondrial ATP synthase)

For immunohistochemistry, brain sections were prepared as described above, hydrated and blocked with 1% BSA in PBS. Sections were incubated at room temperature (25°C) for 1 h with a 1:200 dilution of a rabbit polyclonal antibody (generously provided by Dr E.F. Neufeld, Department of Biological Chemistry, David Geffen School of Medicine at UCLA, Los Angeles, CA, U.S.A.) that was raised against a peptide corresponding to the N-terminus of the mature SCMAS [13]. After washing, SCMAS was visualized using a combined biotinylated goat-anti-rabbit IgG/streptavidin–HRP (horseradish peroxidase)-conjugate detection system (LSAB2 system; Dako) and was viewed under a Nikon E600 microscope.

For detection of SCMAS by Western blotting, 25 μg of protein equivalents of the brain homogenates, prepared as described for the measurement of enzyme activities, were electrophoresed using a Novex Bis-Tris gel (4–12% gradient; Invitrogen) for 35 min at 200 V using Mes buffer (Invitrogen), and were then transferred on to nitrocellulose membrane. SCMAS was probed with a 1:3000 dilution of the rabbit polyclonal antibody and a 1:2500 dilution of goat anti-rabbit IgG (Sigma) labelled with ^{125}I. Radioactivity was measured using phosphoimaging (Typhoon 9400; GE Healthcare). The signal corresponding to SCMAS was determined and corrected for background using ImageQuant 5.2 software (GE Healthcare).

RESULTS AND DISCUSSION

In the present study, we have explored an approach to treat LINCL that does not rely upon restoring the missing TPPI. Instead, we have investigated whether another lysosomal protease, DPPI, can compensate for the loss of TPPI as proposed by Bernardini and Warburton [6]. If this were the case, then small-molecule approaches designed to stimulate endogenous DPPI activity or recombinant methods to provide additional, exogenous DPPI could conceivably provide a valuable adjunct to other therapies. To test whether TPPI and DPPI have compensatory functions *in vivo*, we used a genetic approach in which the mouse model of LINCL was engineered to overexpress or lack DPPI with the expectation that, if there was functional overlap, this would ameliorate or exacerbate disease respectively.

Generation of mutant mice

To determine whether DPPI could functionally compensate for TPPI, our approach was to compare the disease phenotype of mice that lacked either protease with mice that lacked both. Our rationale was that if DPPI could compensate for the loss of TPPI to some extent, then the phenotype of the double mutant would be predicted to be more severe than that of the single TPPI mutant. *Tpp1* and *Ctsc* are both located on mouse chromosome 7 and do not segregate independently, which necessitated the following breeding strategy. Initially, $Tpp1^{-/-}$ mice (mixed 129/SvEv C57BL/6 background) were crossed with $Ctsc^{-/-}$ mice (C57BL/6 background). The double heterozygous F1 progeny were then interbred until crossing-over events generated offspring with a double-mutant haplotype. $Ctsc^{+/-}Tpp1^{-/-}$ males were crossed with $Ctsc^{-/-}Tpp1^{+/-}$ females to obtain $Ctsc^{+/-}Tpp1^{+/-}$, $Ctsc^{-/-}Tpp1^{+/-}$, $Ctsc^{+/-}Tpp1^{-/-}$ and $Ctsc^{-/-}Tpp1^{-/-}$ animals representing control, DPPI deficient, TPPI deficient and DPPI/TPPI double-deficient groups respectively. Genotype analysis revealed that the progeny had roughly the expected Mendelian ratio of 1:1:1:1 (Table 1), indicating that homozygosity for either or both mutant alleles did not result in embryonic lethality.

Enzyme activities in mutant mice

DPPI and TPPI enzyme activities were measured in kidney, heart and brain of the control $Ctsc^{+/-}Tpp1^{+/-}$ animals (Figure 1A). DPPI was found to be highest in kidney and lowest in brain (~9% of kidney activity) which is in accordance with previous transcript abundance [14] and enzyme activity [6] measurements. TPPI activity was also highest in kidney. DPPI and TPPI activities were also measured in the mutant mice and were deficient as predicted in the double mutant and respective single mutants (Figures 1B–1D).

It is worth noting that in the TPPI-deficient animals, DPPI activity was elevated approx. 2-fold in all three tissues examined. In contrast, there was no elevation of TPPI activity in the absence of DPPI. The significance of the increase in DPPI activity in the absence of TPPI is not clear, but it could indicate that there is an up-regulation of DPPI synthesis as a cellular response to the loss of TPPI, suggesting that DPPI may compensate for some aspect of TPPI function. Alternatively, given that progressive reactive gliosis occurs in the TPPI-deficient mouse [15] and that DPPI plays a role in immune function, it is possible that the increased levels of DPPI observed in these mice may simply reflect a CNS inflammatory response

rather than a neuronal effort to compensate for the loss of TPPI. This effect could be accentuated by a change in the distribution of CNS cell types as neurons are lost.

Lysosomal storage in the mutant mice

The accumulation of autofluorescent storage material is a histological hallmark of LINCL and is a prominent feature of the brain of the *Tpp1*-targeted mouse [4]. At 112–119 days, autofluorescent cytoplasmic storage material was observed at similar levels in both the TPPI-deficient and the DPPI/TPPI double-deficient animals in various brain regions including the hippocampus, thalamus and cortex (Figure 2). Little or no fluorescent storage material was observed in the control or single DPPI-deficient groups (Figure 2).

A major component of the storage material in LINCL and other NCLs is the small proteolipid, SCMAS [16] and an accumulation of this protein in NCLs can be demonstrated immunohistochemically [17]. As a measure of disease progression, we conducted immunohistochemical staining for SCMAS in the single- and double-mutant mice (Figure 3A). Both TPPI-deficient and DPPI/TPPI double-deficient brain stained strongly for SCMAS, but there was no staining in the control and single DPPI-deficient brains.

In order to quantify the levels of SCMAS in the brains of the mutant mice, immunoblotting was performed using whole brain homogenates (Figure 3B). The amount of SCMAS in brain was equally elevated approx. 4-fold in both the TPPI-deficient and the double-deficient groups compared with either the control or the single DPPI-deficient group, a result that is consistent with the immunohistochemistry (Figure 3A).

SCMAS may represent a direct substrate of TPPI [18] and, based on primary sequence considerations alone, should be a direct substrate of both TPPI and DPPI [19–23]. However, it is possible that factors other than sequence alone are important for intralysosomal hydrolysis of SCMAS *in vivo*. Alternatively, it may be relevant that recent detailed substrate specificity studies on TPPI indicate that this enzyme can readily hydrolyse model substrates with basic N-termini as well as substrates with a proline at residue N+1 [22]. Such peptides are poor substrates for DPPI [19–21]. Thus intrinsic differences in substrate specificity may explain, in part, the inability for DPPI to functionally compensate for TPPI.

We also investigated whether the absence of extraneural pathology in LINCL is due to the presence of DPPI that can compensate for the absence of TPPI. Kidney has relatively high levels of both enzyme activities and thus was examined in detail. Autofluorescence and haematoxylin and eosin staining revealed a lack of apparent pathology in the single- or double-mutant animals (Figure 4, top and middle panels). Similar analysis of liver and heart also failed to reveal accumulation of storage material (results not shown).

Despite the absence of obvious storage material, the loss of TPPI does have an observable effect in kidney. In the present study, while there was detectable immunohistochemical staining for SCMAS in control kidney, staining was greater in the TPPI single mutant and the DPPI/TPPI double mutant (Figure 4, bottom panels). In contrast, SCMAS staining in the DPPI single mutant appeared identical with controls. The finding that the absence or presence of DPPI has no significant effect on SCMAS accumulation due to a loss of TPPI

provides a further indication that DPPI is not likely to have overlapping function with TPPI *in vivo*.

Survival of the mutant mice

We previously found that TPPI-deficient mice have a greatly shortened lifespan, with a median survival of 138 days [4]. In the present study, in a mixed C57BL/6 and 129Sv genetic background, the single TPPI-deficient group had a median survival of 121 days. This was not significantly different from the 131 day median survival of the double-deficient group (Figure 5) as determined by either log-rank or the Gehan–Breslow–Wilcoxon Test (results not shown). Disease in single TPPI-deficient animals starts with the onset of tremors at approx. 7 weeks of age that progressively worsens over time and is eventually accompanied by ataxia. There was no obvious deviation from this disease course in the double-mutant mice.

Transgenic expression of DPPI in the brain of *Tpp1* mutant mice

The additional loss of DPPI appeared to have no significant effect on disease course in the TPPI-deficient mouse, suggesting that there is no compensatory function *in vivo*. However, it is possible that the endogenous DPPI activity in neurons is so low compared with peripheral tissues that eliminating this activity from the TPPI-deficient brain may have little or no additional pathogenic effect. Thus, in addition to determining whether a loss of DPPI exacerbates disease, we also conducted a direct test of whether increasing levels of DPPI in the brain might attenuate disease. This was achieved by the generation of a transgenic mouse where expression of the human CTSC cDNA is regulated by the rat NSE promoter (DPPI transgene) (Figure 6A). Two founders, 43416 and 43437, were identified by Southern blot analysis (Figure 6B) and were crossed with *Tpp1*-targeted mice to generate transgenic mice in a TPPI-deficient background. Brains of the transgenic mice from both lines showed a 2-fold increase in DPPI activity but there was little or no significant increase in DPPI activity in peripheral tissues such as kidney and heart (Figure 6C), consistent with the expected expression of the neuronal-specific transgene promoter.

Effect of expression of transgenic DPPI on disease phenotype in the TPPI mutant

DPPI activities were measured in the brains of the TPPI-deficient mice in the presence or absence of the DPPI transgene (Figure 7A). As observed previously (Figure 1), endogenous DPPI levels were increased approx. 2-fold in the absence of TPPI in mice that lacked the DPPI transgene. However, in the TPPI mutants that contained the transgene, DPPI levels in brain were over 4-fold higher than the control endogenous activity. Despite the increased levels of DPPI, SCMAS accumulation arising from the TPPI-deficiency was not ameliorated by the presence of the transgene (Figure 7B). In accordance with this, levels of autofluorescent storage material were similar in TPPI mutants with or without the transgene (results not shown). Taken together, these results indicate that increased levels of DPPI in brain do not reduce the cellular pathology associated with LINCL. Consistent with this lack of improvement, survival analysis of both independent transgenic lines indicated that that the additional DPPI activity within the brain failed to increase the life-span of the TPPI-deficient animals (Figure 8).

Concluding Remarks

LINCL is a fatal lysosomal storage disorder of children and currently there is no effective treatment for this disease. However, there is some promising progress in several therapeutic directions that are designed to replace the missing enzyme, TPPI. AAV (adeno-associated virus)-mediated gene therapy has been used to successfully rescue the disease phenotype in the *Tpp1*-targeted mouse model of LINCL [24–26] and viral-mediated gene replacement therapy (www.clinicaltrials.gov/ct2/show/NCT00151216) has been conducted in affected children [27]. In addition, enzyme-replacement therapy to the brain of affected *Tpp1*-targeted mice indicate that this approach may also have potential [15]. Although the clearest treatment for LINCL would be to replace the missing TPPI activity, there are currently formidable obstacles to such approaches, particularly in terms of delivering large molecules to the brain. In the present study, we have therefore investigated another approach which would rely on the ability of another enzyme, DPPI, to functionally compensate for the loss of TPPI. Our results suggest that this will not be a useful strategy; genetic manipulations that either increased DPPI in neurons by at least 2-fold or that completely abolished the enzyme in all tissues did not significantly influence disease progression or pathology in the *Tpp1*-targeted mice.

Although our results indicate that increasing DPPI activity would probably not result in therapeutic benefits in LINCL, the approach of augmenting a compensatory activity may still have potential. However, in order to identify candidates for such an activity, it will be necessary to have a clear understanding of the composition of the storage material in LINCL and the physiological substrates of TPPI.

Acknowledgments

This work was supported by National Institutes of Health Grant NS37918 (to P. L.) and a research fellowship (to K.-H.K.) from the Batten Disease Support and Research Association. We would like to thank Dr Elizabeth Neufeld, Dr J. Gregor Sutcliffe and Dr Curt Sigmund for generously providing reagents and Dr Donald Winkelmann and Dr Karel RaŠka, Jr (University of Medicine and Dentistry of New Jersey, Robert Wood Johnson Medical School, Piscataway, NJ, U.S.A.) for their help with the histological studies.

Abbreviations used

AMC	7-amino-4-methylcoumarin
CNS	central nervous system
DPPI	dipeptidyl-peptidase I
LINCL	late-infantile neuronal ceroid lipofuscinosis
NCL	neuronal ceroid lipofuscinosis
NSE	neuron-specific enolase
SCMAS	subunit c of mitochondrial ATP synthase
TPPI	tripeptidyl-peptidase I

REFERENCES

1. Goebel, HH.; Mole, SE.; Lake, BD. Neuronal Ceroid Lipofuscinoses (Batten Disease). Amsterdam: IOS Press; 1999.
2. Sleat DE, Donnelly RJ, Lackland H, Liu CG, Sohar I, Pullarkat RK, Lobel P. Association of mutations in a lysosomal protein with classical late-infantile neuronal ceroid lipofuscinosis. Science. 1997; 277:1802–1805. [PubMed: 9295267]
3. Sohar, I.; Sleat, DE.; Lobel, P. Tripeptidyl-peptidase. I. In: Barrett, AJ.; Rawlings, ND.; Woessner, JF., editors. Handbook of Proteolytic Enzymes. London: Academic Press; 2004. p. 1893-1896.
4. Sleat DE, Wiseman JA, El-Banna M, Kim KH, Mao Q, Price S, Macauley SL, Sidman RL, Shen MM, Zhao Q, et al. A mouse model of classical late-infantile neuronal ceroid lipofuscinosis based on targeted disruption of the CLN2 gene results in a loss of tripeptidyl-peptidase I activity and progressive neurodegeneration. J. Neurosci. 2004; 24:9117–9126. [PubMed: 15483130]
5. Du PG, Kato S, Li YH, Maeda T, Yamane T, Yamamoto S, Fujiwara M, Yamamoto Y, Nishi K, Ohkubo I. Rat tripeptidyl peptidase I: molecular cloning, functional expression, tissue localization and enzymatic characterization. Biol. Chem. 2001; 382:1715–1725. [PubMed: 11843185]
6. Bernardini F, Warburton MJ. Lysosomal degradation of cholecystokinin-(29–33)-amide in mouse brain is dependent on tripeptidyl peptidase-I: implications for the degradation and storage of peptides in classical late-infantile neuronal ceroid lipofuscinosis. Biochem. J. 2002; 366:521–529. [PubMed: 12038963]
7. Adkison AM, Raptis SZ, Kelley DG, Pham CT. Dipeptidyl peptidase I activates neutrophil-derived serine proteases and regulates the development of acute experimental arthritis. J. Clin. Invest. 2002; 109:363–371. [PubMed: 11827996]
8. Pham CT, Ley TJ. Dipeptidyl peptidase I is required for the processing and activation of granzymes A and B *in vivo*. Proc. Natl. Acad. Sci. U.S.A. 1999; 96:8627–8632. [PubMed: 10411926]
9. Sheth PD, Pedersen J, Walls AF, McEuen AR. Inhibition of dipeptidyl peptidase I in the human mast cell line HMC-1: blocked activation of tryptase, but not of the predominant chymotryptic activity. Biochem. Pharmacol. 2003; 66:2251–2262. [PubMed: 14609749]
10. Pham CT, Armstrong RJ, Zimonjic DB, Popescu NC, Payan DG, Ley TJ. Molecular cloning, chromosomal localization, and expression of murine dipeptidyl peptidase. I. J. Biol. Chem. 1997; 272:10695–10703. [PubMed: 9099719]
11. Hart TC, Hart PS, Bowden DW, Michalec MD, Callison SA, Walker SJ, Zhang Y, Firatli E. Mutations of the cathepsin C gene are responsible for Papillon–Lefevre syndrome. J. Med. Genet. 1999; 36:881–887. [PubMed: 10593994]
12. Stec DE, Morimoto S, Sigmund CD. Vectors for high-level expression of cDNAs controlled by tissue-specific promoters in transgenic mice. Biotechniques. 2001; 31:256–258. [PubMed: 11515356]
13. Ryazantsev S, Yu WH, Zhao HZ, Neufeld EF, Ohmi K. Lysosomal accumulation of SCMAS (subunit c of mitochondrial ATP synthase) in neurons of the mouse model of mucopolysaccharidosis III B. Mol. Genet. Metab. 2007; 90:393–401. [PubMed: 17185018]
14. Rao NV, Rao GV, Hoidal JR. Human dipeptidyl-peptidase. I. Gene characterization, localization, and expression. J. Biol. Chem. 1997; 272:10260–10265. [PubMed: 9092576]
15. Chang M, Cooper JD, Sleat DE, Cheng SH, Dodge J, Passini M, Lobel P, Davidson BL. Intraventricular enzyme replacement improves disease phenotypes in a mouse model of late infantile neuronal ceroid lipofuscinosis. Mol. Ther. 2008; 16:649–656. [PubMed: 18362923]
16. Palmer DN, Martinus RD, Cooper SM, Midwinter GG, Reid JC, Jolly RD. Ovine ceroid lipofuscinosis. The major lipopigment protein and the lipid-binding subunit of mitochondrial ATP synthase have the same NH2-terminal sequence. J. Biol. Chem. 1989; 264:5736–5740. [PubMed: 2522438]
17. Hosain S, Kaufmann WE, Negrin G, Watkins PA, Siakotos AN, Palmer DN, Naidu S. Diagnoses of neuronal ceroid-lipofuscinosis by immunochemical methods. Am. J. Med. Genet. 1995; 57:239–245. [PubMed: 7668338]

18. Ezaki J, Takeda-Ezaki M, Kominami E. Tripeptidyl peptidase. I. the late infantile neuronal ceroid lipofuscinosis gene product, initiates the lysosomal degradation of subunit c of ATP synthase. J. Biochem. 2000; 128:509–516. [PubMed: 10965052]

19. McDonald JK, Callahan PX, Zeitman BB, Ellis S. Inactivation and degradation of glucagon by dipeptidyl aminopeptidase I (cathepsin C) of rat liver. J. Biol. Chem. 1969; 244:6199–6208. [PubMed: 5389103]

20. McDonald JK, Zeitman BB, Reilly TJ, Ellis S. New observations on the substrate specificity of cathepsin C (dipeptidyl aminopeptidase I). Including the degradation of β-corticotropin and other peptide hormones. J. Biol. Chem. 1969; 244:2693–2709. [PubMed: 4306035]

21. McGuire MJ, Lipsky PE, Thiele DL. Purification and characterization of dipeptidyl peptidase I from human spleen. Arch. Biochem. Biophys. 1992; 295:280–288. [PubMed: 1586157]

22. Tian Y, Sohar I, Taylor JW, Lobel P. Determination of the substrate specificity of tripeptidyl-peptidase I using combinatorial peptide libraries and development of improved fluorogenic substrates. J. Biol. Chem. 2006; 281:6559–6572. [PubMed: 16339154]

23. Doebber TW, Divor AR, Ellis S. Identification of a tripeptidyl aminopeptidase in the anterior pituitary gland: effect on the chemical and biological properties of rat and bovine growth hormones. Endocrinology. 1978; 103:1794–1804. [PubMed: 748018]

24. Cabrera-Salazar MA, Roskelley EM, Bu J, Hodges BL, Yew N, Dodge JC, Shihabuddin LS, Sohar I, Sleat DE, Scheule RK, et al. Timing of therapeutic intervention determines functional and survival outcomes in a mouse model of late infantile Batten disease. Mol. Ther. 2007; 15:1782–1788. [PubMed: 17637720]

25. Passini MA, Dodge JC, Bu J, Yang W, Zhao Q, Sondhi D, Hackett NR, Kaminsky SM, Mao Q, Shihabuddin LS, et al. Intracranial delivery of CLN2 reduces brain pathology in a mouse model of classical late infantile neuronal ceroid lipofuscinosis. J. Neurosci. 2006; 26:1334–1342. [PubMed: 16452657]

26. Sondhi D, Hackett NR, Peterson DA, Stratton J, Baad M, Travis KM, Wilson JM, Crystal RG. Enhanced survival of the LINCL mouse following CLN2 gene transfer using the rh.10 Rhesus Macaque-derived adeno-associated virus vector. Mol. Ther. 2007; 15:481–491. [PubMed: 17180118]

27. Worgall S, Sondhi D, Hackett NR, Kosofsky B, Kekatpure MV, Neyzi N, Dyke JP, Ballon D, Heier L, Greenwald BM, et al. Treatment of late infantile neuronal ceroid lipofuscinosis by CNS administration of a serotype 2 adeno-associated virus expressing CLN2 cDNA. Hum. Gene. Ther. 2008; 19:463–474. [PubMed: 18473686]

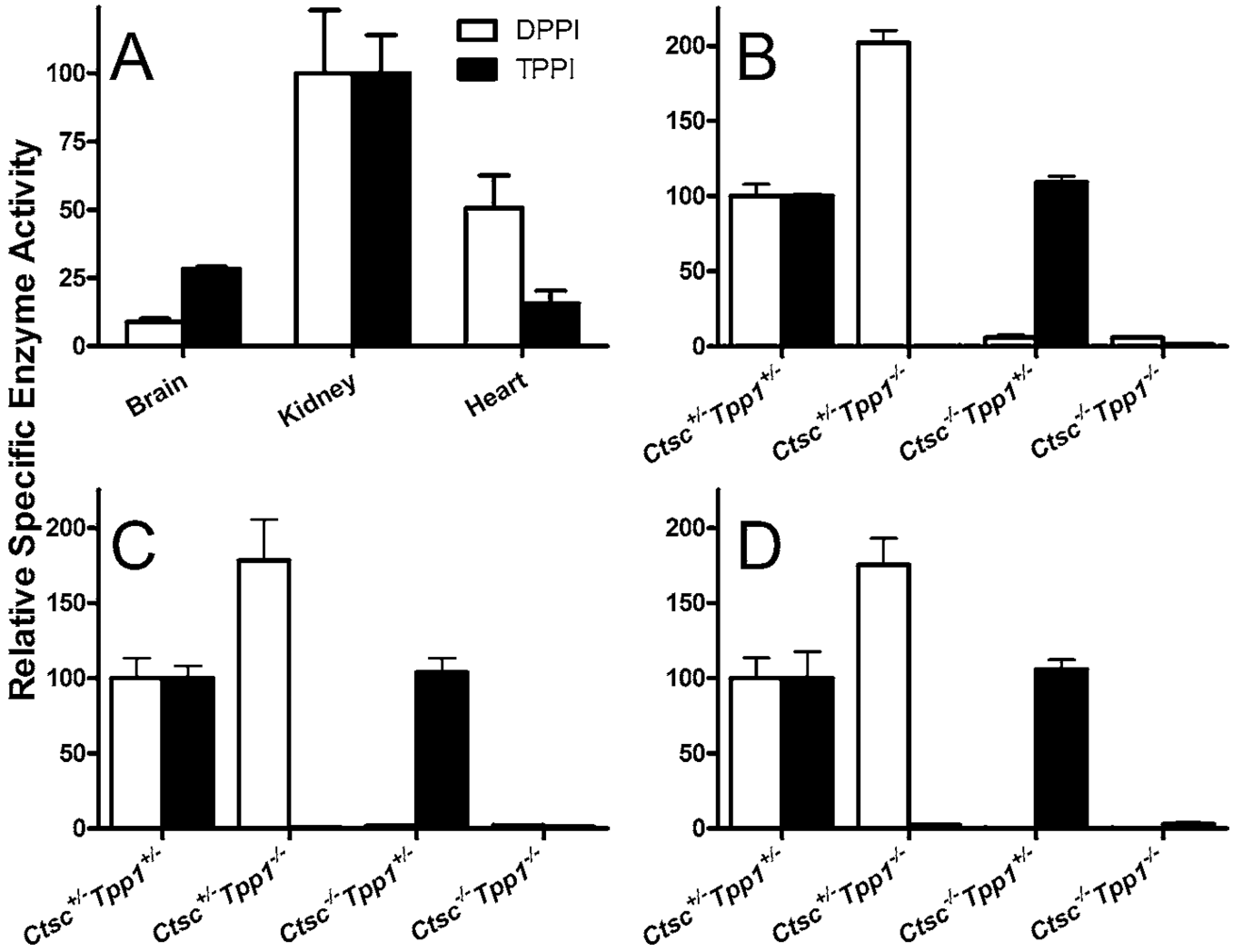

Figure 1. TPPI and DPPI enzyme activities in mutant mice

Mice were 112–119 days old. Each column represents the mean DPPI or TPPI enzyme activity normalized to control kidney with error bars showing the S.E.M. (n = 2 or 3 animals per group). (**A**) Activity from control mice ($Ctsc^{+/-}Tpp1^{+/-}$) in different tissues, normalized to the activity of each enzyme in the kidney. (**B–D**) show enzyme activities of different genotype animals normalized to the control in brain (**B**), kidney (**C**) and heart (**D**).

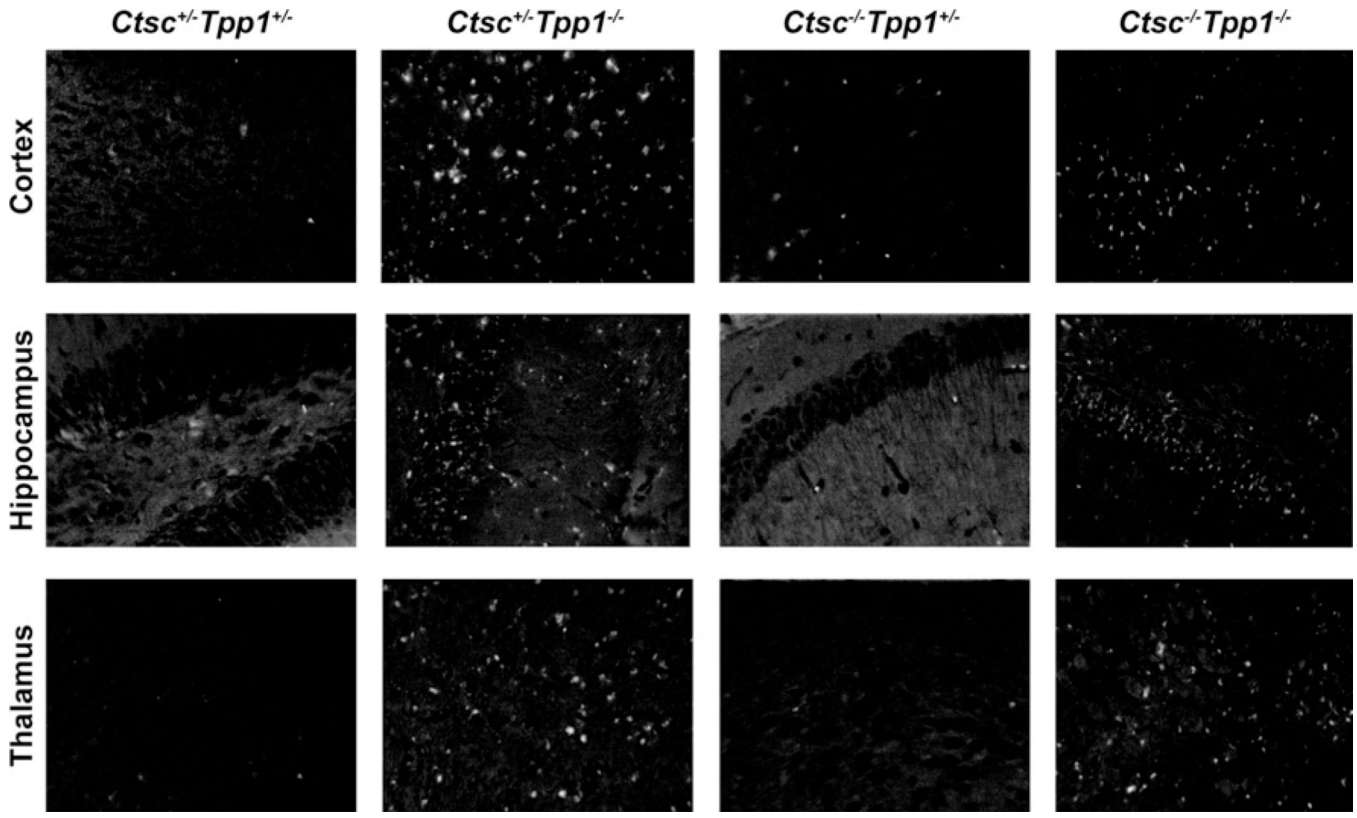

Figure 2. Analysis of brain autofluorescent storage material in control and mutant mice

Genotypes and brain regions of animals are indicated for each panel. Mice were 112–119 days old and images were obtained at 20 × magnification.

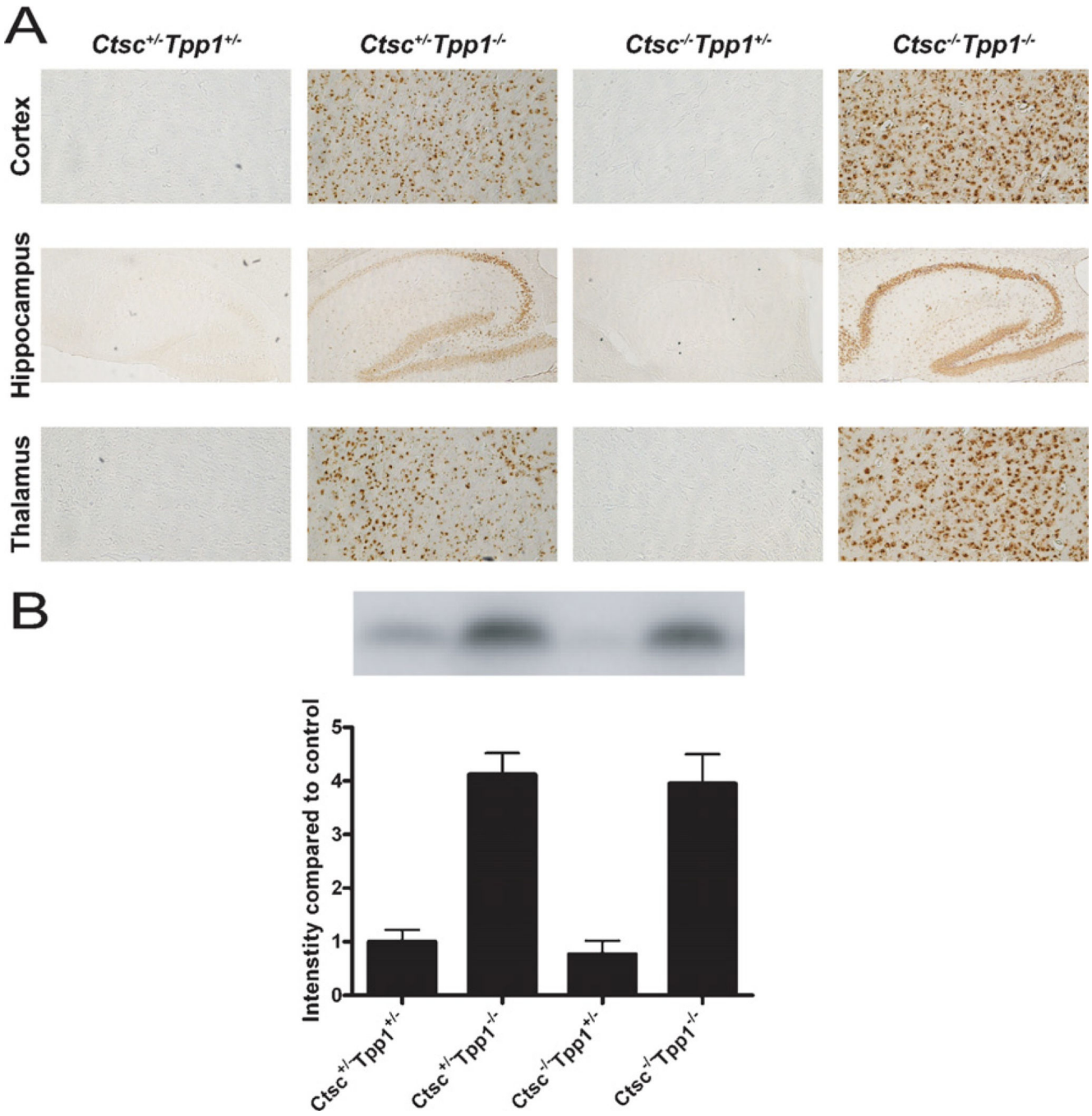

Figure 3. Accumulation of SCMAS in control and mutant mice

(**A**) Immunohistochemical analysis of different CNS regions. Mice were 125 days old and images were obtained at 10 × magnification for hippocampus and 40 × for cortex and thalamus. (**B**) Western blotting of mouse brain homogenates. Each column represents the mean SCMAS levels in two animals and error bars represent the range.

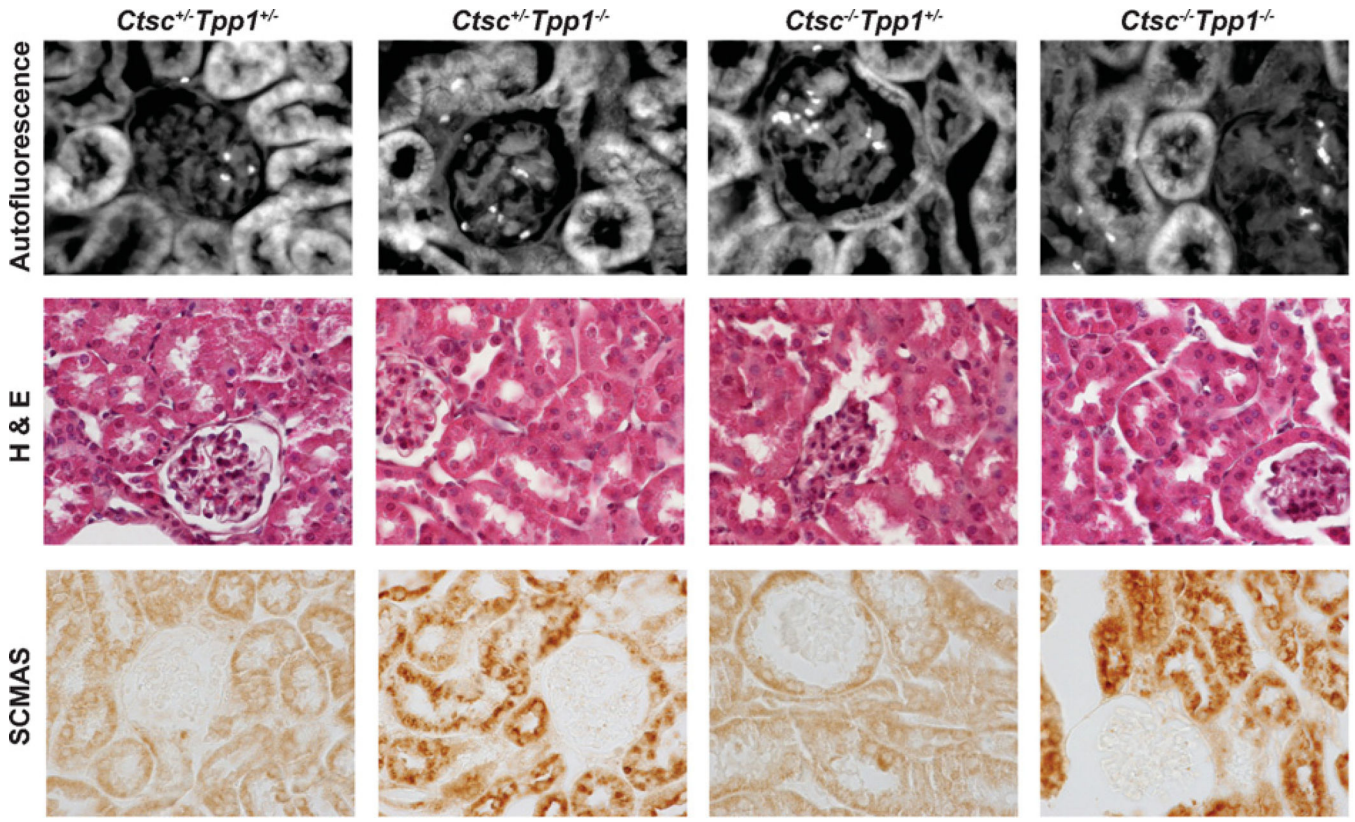

Figure 4. Histological analysis of control and mutant mouse kidneys

Mice were 125 days old and images were obtained at 60 × magnification. H&E, haematoxylin and eosin.

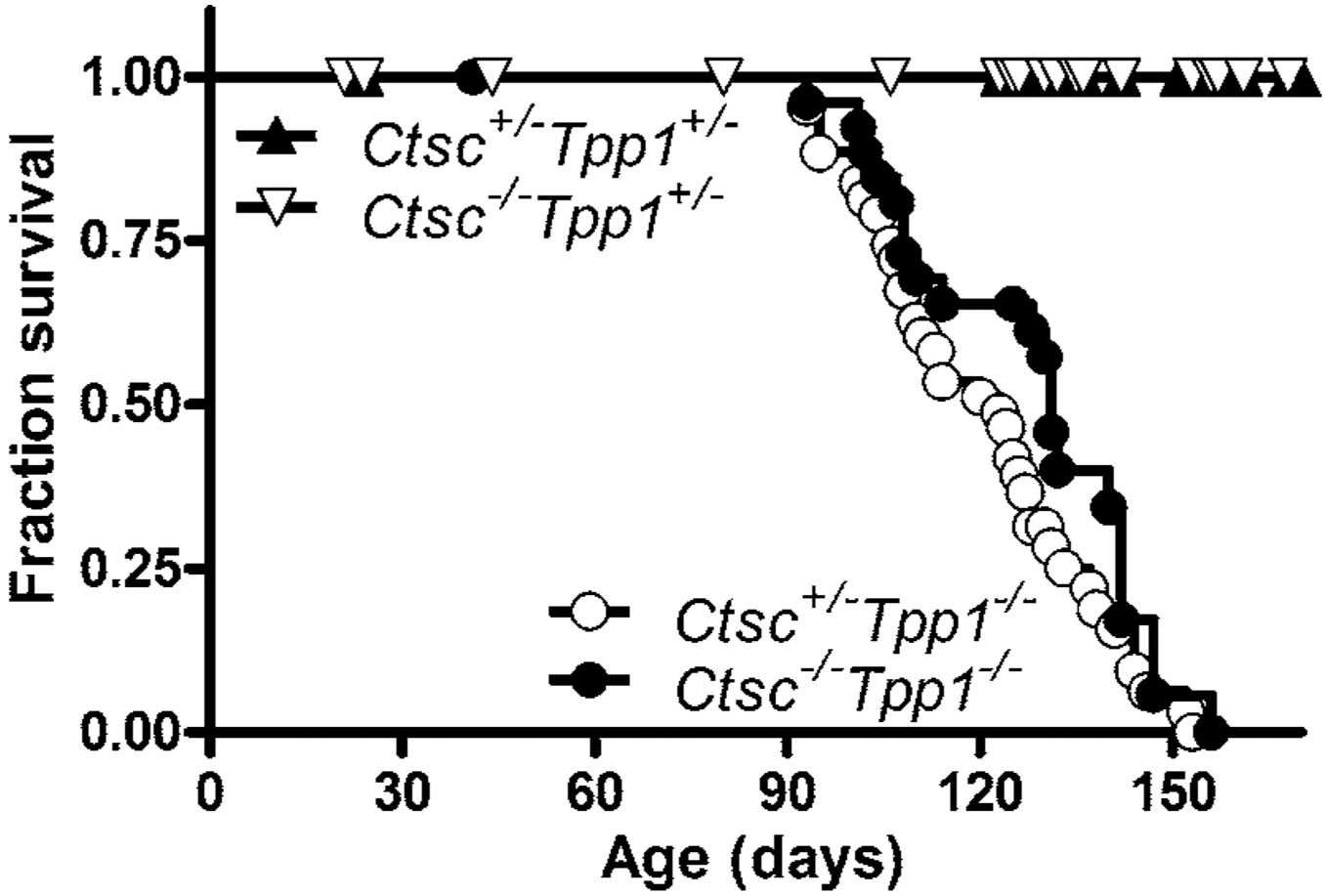

Figure 5. Survival of mice with deficiencies in DPPI and/or TPPI

The number of animals analysed were as follows: *Ctsc*$^{+/-}$ *Tpp1*$^{+/-}$, *n* = 31; *Ctsc*$^{-/-}$ *Tpp1*$^{+/-}$, *n* = 44; *Ctsc*$^{+/-}$ *Tpp1*$^{-/-}$, *n* = 43; and *Ctsc*$^{-/-}$ /*Tpp1*$^{-/-}$, *n* = 27.

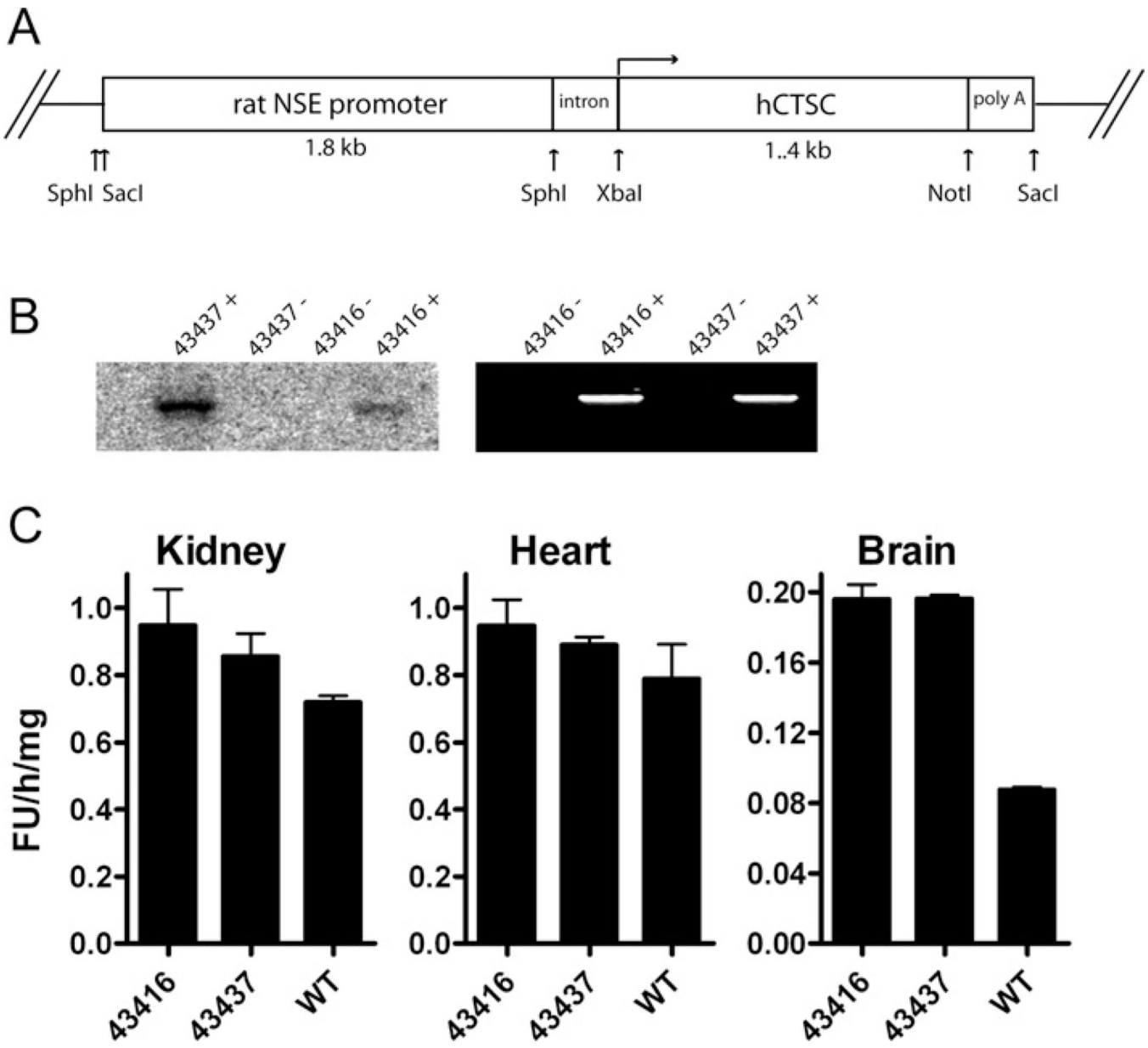

Figure 6. Transgenic expression of DPPI

(**A**) Schematic of the transgenic construct designed to express DPPI within the CNS under the regulation of the NSE promoter. (**B**) Genotyping of transgenic mice by Southern blotting (left-hand panel) or by PCR amplification (right-hand panel) as described in the Experimental section. (**C**) DPPI activity in kidney, heart and brain from two independent founder lines and wild-type controls. Mice were 60 days old. Each column represents the mean DPPI enzyme activity [arbitrary fluorescent units (FU)/h per mg of protein) with error bars showing the S.E.M. (n = 3 animals per group).

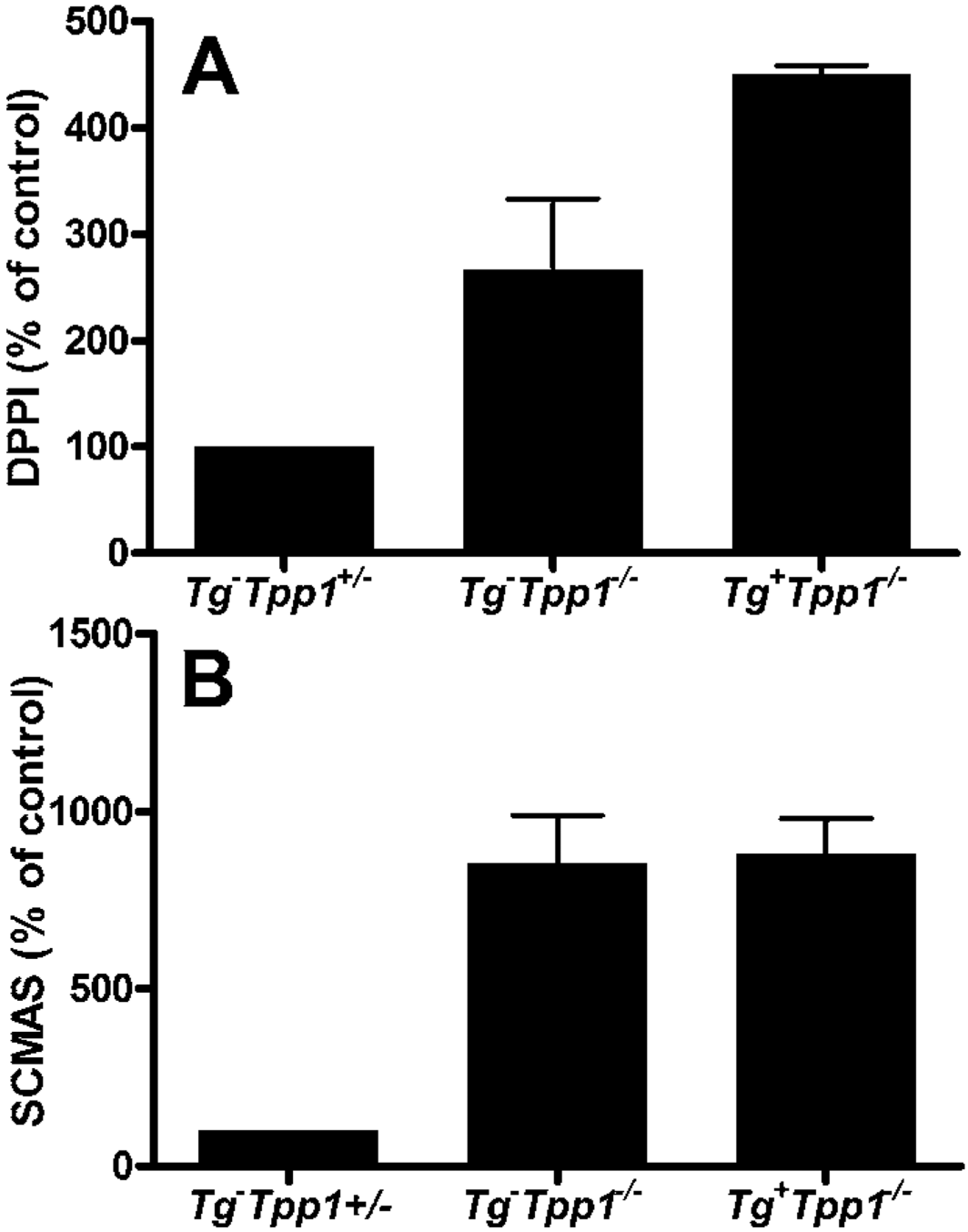

Figure 7. Effects of increased DPPI expression in TPPI-deficient mouse brain

DPPI activity (**A**) or SCMAS levels (**B**) in TPPI-deficient littermates lacking or containing the CTSC transgene (line 43437) was compared with age-matched ~125-day-old controls. Each column represents the mean DPPI enzyme activity or SCMAS level normalized to the $Tg^{-}Tpp1^{+/-}$ control with error bars showing the range (n = 2 or 3 animals per group).

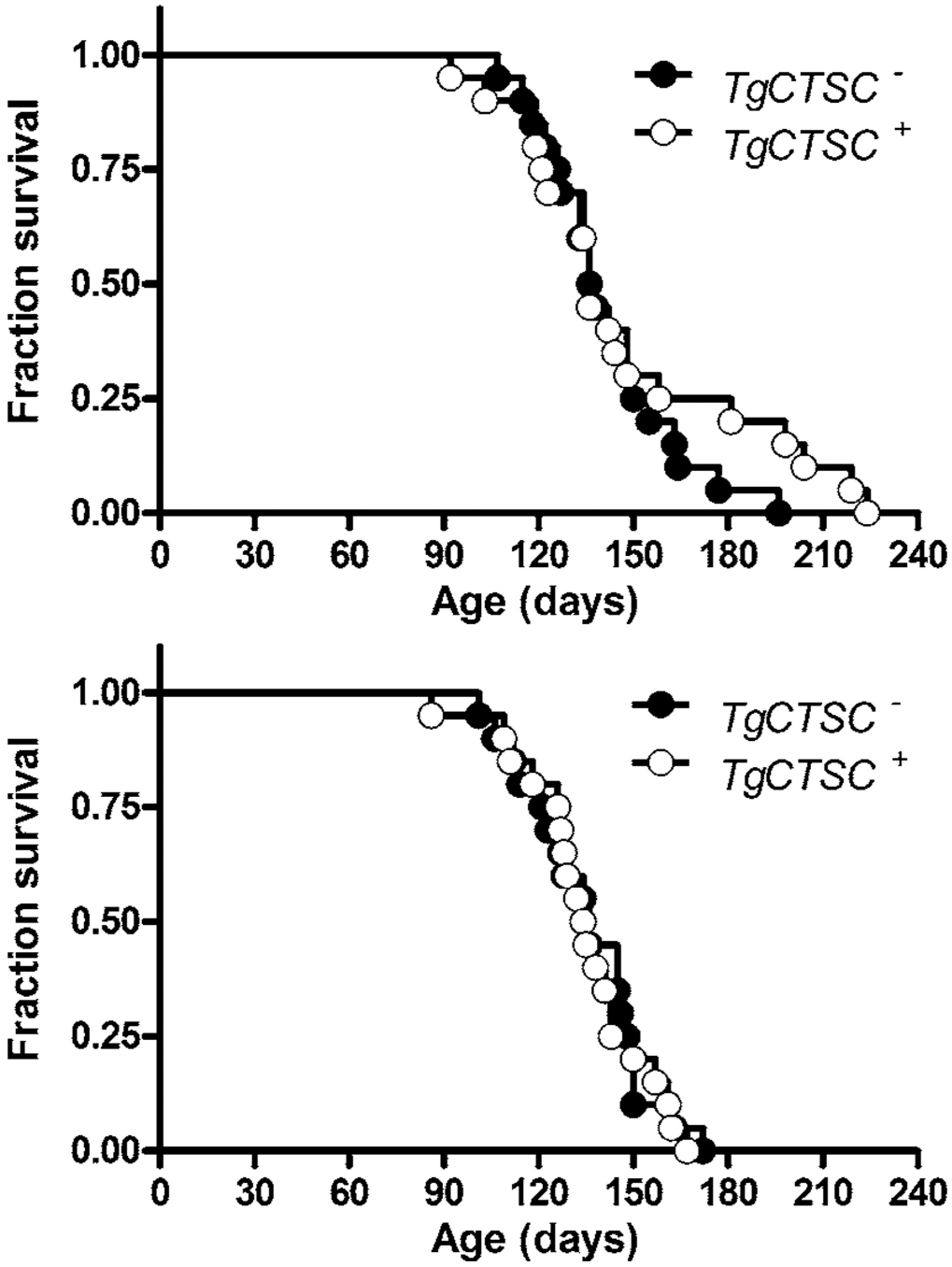

Figure 8. Effect of transgenic expression of DPPI on survival of TPPI-deficient mice

Values are shown for the two independent transgenic lines. The top panel shows transgenic line 43416 and littermate controls. The bottom panel shows transgenic line 43437 and littermate controls. Each group contained 20 animals.

Table 1

Progeny from male *Ctsc*$^{+/-}$*Tpp1*$^{-/-}$ × female *Ctsc*$^{-/-}$*Tpp1*$^{+/-}$ matings

The distribution of observed genotypes was compared with the expected Mendelian distribution. One-way χ^2 test indicates that there is no significant difference between observed and expected frequencies ($P = 0.4137$).

Distribution	*Ctsc*$^{+/-}$*Tpp1*$^{+/-}$	*Ctsc*$^{+/-}$*Tpp1*$^{-/-}$	*Ctsc*$^{-/-}$*Tpp1*$^{+/-}$	*Ctsc*$^{-/-}$*Tpp1*$^{-/-}$
Observed	42	51	59	52
Expected	51	51	51	51